GSI-Preprint-99-13
April 1999

SECONDARY PION BEAMS AT GSI

R.S. Simon for the PION collaboration
M. Alvarez, M. Ardid, V. Avdeichikov, F. Ballester, H. Bokemeyer, L. Carlen, J. Díaz, O. Hartmann, B. Jakobsson, W. Koenig, B. Krusche, U. Leinberger, B. Lommel, V. Metag, W. Mittig, Y. Murin, R. Novotny, W. Niebur, R. Schicker, W. Schön, A. Schröter, R.S. Simon, N. Yahlali

Gesellschaft für Schwerionenforschung mbH
Planckstraße 1 • D-64291 Darmstadt • Germany
Postfach 11 05 52 • D-64220 Darmstadt • Germany

Secondary Pion Beams at GSI

R.S. Simon for the PION collaboration

M. Alvarez[1], M. Ardid[1], V. Avdeichikov[2], F. Ballester[1], H. Bokemeyer[3], L. Carlen[2], J. Díaz[1], O. Hartmann[4], B. Jakobsson[2], W. Koenig[3], B. Krusche[4], U. Leinberger[3], B. Lommel[3], V. Metag[3], W. Mittig[5], Y. Murin[2], R. Novotny[4], W. Niebur[3], R. Schicker[3] W. Schön[3], A. Schröter[3], R.S. Simon[3], N. Yahlali[1]

[1]IFIC, Centro Mixto Universidad de Valencia–CSIC, E-46100 Burjassot, Spain
[2]Department of Physics, University of Lund, S-22362 Lund, Sweden
[3]Gesellschaft für Schwerionenforschung, D-64291 Darmstadt, Germany
[4]II. Physikalisches Institut, Universität Gießen, D-35392 Gießen, Germany
[5]Grand Accélérateur National d'Ions Lourds, F-14021 Caen Cedex, France

Abstract

Protons and ^{12}C ions from the 18 Tm synchrotron have been used to irradiate a production target of beryllium, with the resulting pion beams being transported to the nearest downstream experimental area. The beam line accomodates pion momenta up to 2.8 GeV/c and has a momentum acceptance of 8%. For ^{12}C projectiles with the maximum energy of $2A$ GeV the negative pion yields reach values of 1×10^7/spill near the peak of the momentum distribution around 1 GeV/c, if extrapolated to the space charge limit of the synchrotron. The corresponding p–induced yields at 3.5 GeV are smaller except for hard pions for which the production exceeds the ^{12}C–induced intensities because of the higher energy per nucleon.

1 Introduction

Research synchrotrons routinely offer beams of secondary particles in addition to their primary projectiles. One example is the C6/C8 low–energy separated beam line of the Brookhaven AGS which provides π^+ and π^- intensities up to 10^8/spill at 700 MeV/c momentum. Other examples are the K6 beam line of the 12 GeV proton synchrotron at KEK with 10^7 pions in the momentum range from 0.6 to 2 GeV/c [1], or the meson facility at the 10 GeV proton synchrotron of ITEP Moscow [2] and the pion beams at the CERN PS and SPS.

Recently a pion beam has also been established at the heavy-ion synchrotron SIS at GSI Darmstadt. The scientific goal of pion experiments at GSI is to broaden the current research program of the laboratory in the field of relativistic heavy–ion collisions. A topic of general interest is the modification of hadron properties in nuclear matter. While strong effects are predicted for the high compression and elevated temperatures reached in nucleus–nucleus collisions, measurable changes should already occur at normal nuclear density and zero temperature and would be accessible in pion–induced reactions. In particular the light vector mesons, ephemeral products of pion–nucleon interactions and predicted to have a propensity for in–medium mass changes, are well within reach of the pion momentum range.

Two unique detector systems are available for these studies. The FOPI detector is capable of charged–particle detection over the full solid angle. It features a central drift chamber surrounded by a time–of–flight and a Čerenkov barrel, all within a solenoidal magnetic field. The HADES experiment on the other hand specializes on electron and positron spectroscopy. Providing a geometrical acceptance for e^+e^- pairs of 20 – 40%, HADES uses a RICH detector for lepton identification and has two inner and two outer planes of drift chambers with an intermediate toroidal magnetic field for particle tracking. For the coincident detection of photons HADES may be augmented by the photon spectrometer TAPS, an array of individual BaF_2 scintillators with a depth of 12 radiation lengths.

2 The Pion Beam Facility

2.1 Floor plan of the SIS target hall

The remote–controlled production target is placed in the main beam line coming from the synchrotron. As shown in fig.1 pions can be delivered to all major experimental areas of the SIS target hall. The line to cave H is the shortest among the secondary beam lines. It was chosen for the commissioning of the pion beam facility.

2.2 Production target and beam line to cave H

The pion production target consists of beryllium. The pencil–like target is clamped in a water–cooled copper block and has a length of 100 mm and a diameter of 7 mm. For better emission of the secondary particles the free end of the target rod is tapering down to 4 mm diameter over the last 30 mm.

Particles leaving the production target are first collected by a pair of quadrupole lenses and then deflected by a dipole bending magnet and focused to an intermediate image plane by means of a second quadrupole doublet (see fig.2). The design–value for the momentum dispersion $\Delta x/(\Delta p/p)$ is – 9 mm/%. Arranged symmetrically to the image plane, the remaining section of the beam line subsequently transports the particles to the experimental target point. Production target and HADES target point are at different elevations. This is taken into account by slightly tilting the two bending magnets with respect to the horizontal plane. While the first magnet adds a vertical component to the beam direction, the second dipole restores the beam to its horizontal trajectory. Altogether the beam rises by 70 cm, reaching a height of 270 cm above the floor. Horizontally the beam is deflected to the left in both dipole magnets (see fig.1).

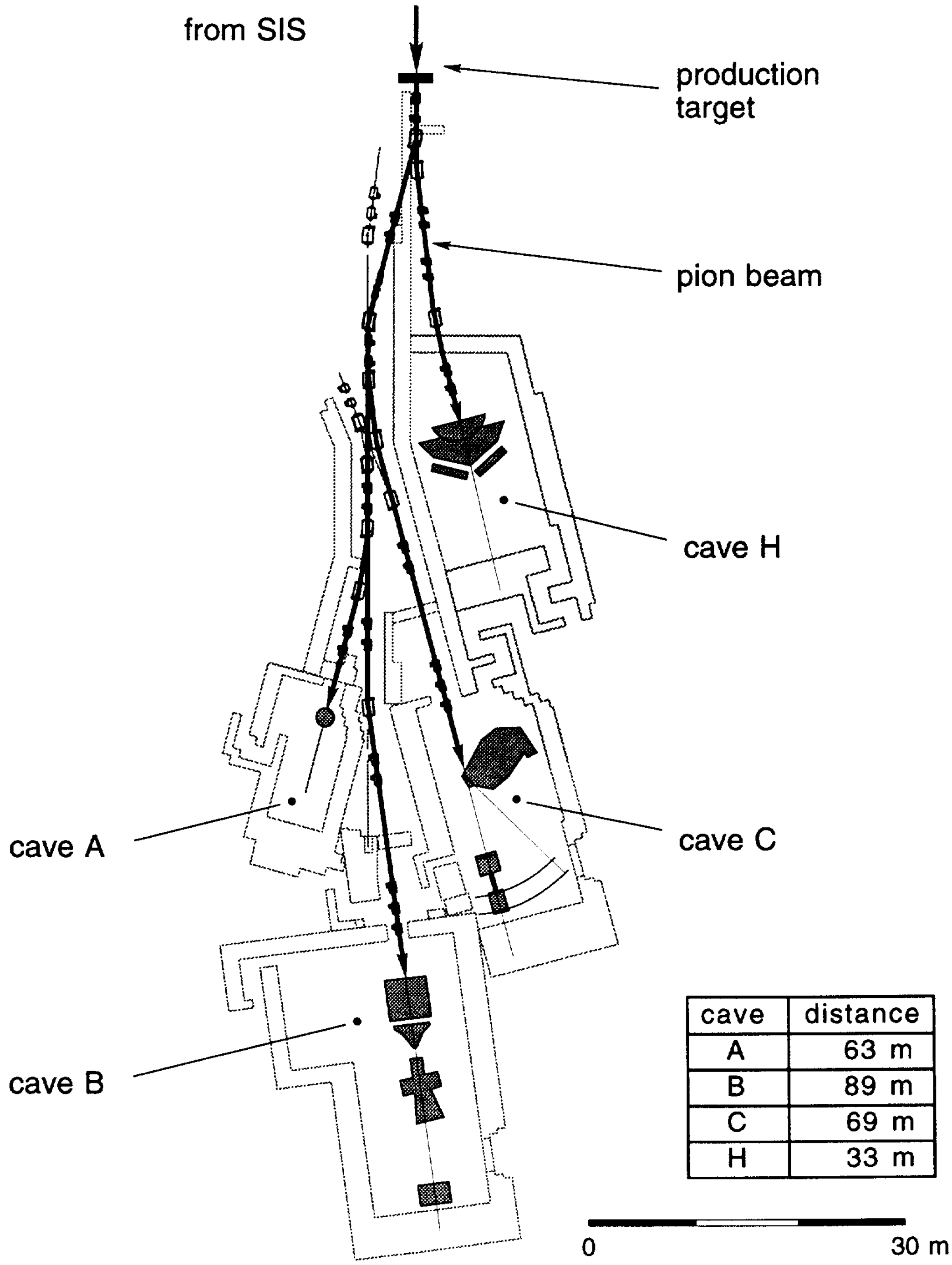

Figure 1: Pion production target and associated beam lines. The FOPI and HADES detectors located in cave B and cave H, respectively, are particularly suited for pion experiments.

The focusing strength of the first quadrupole doublet essentially defines the acceptance of the beam line. Momenta up to 2.8 GeV/c can be accomodated with a solid angle of $\Delta\Omega$ = 2.3 msr and a momentum acceptance of $\Delta p/p$ = 8%. The length L of the beam line is 33 m, resulting in a survival probability of $\exp(-L/\beta\gamma c\tau)$ = 55% for pions with a momentum of 1 GeV/c. The mean life $c\tau$ of pions is 7.804 m.

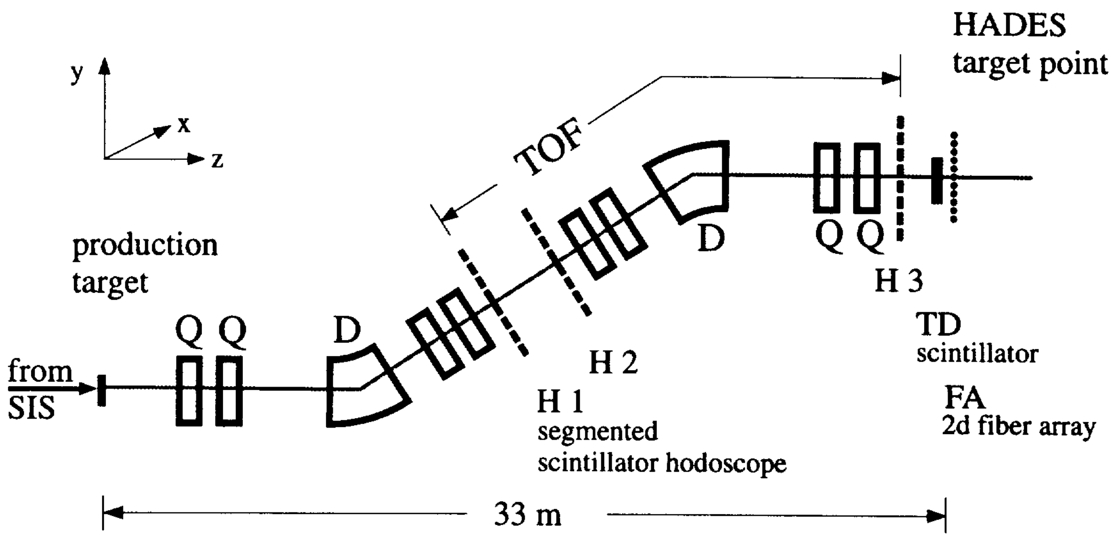

Figure 2: Beam line to cave H (side view, schematic). Between the dipole magnets the beam rises by 70 cm.

2.3 The beam line hodoscopes

Exclusive pion experiments require a momentum definition for the pions which is more accurate than the pre–selected acceptance window of the beam line. In addition, it is necessary to identify the pions among the flux of secondary particles that strike the target. Both tasks are addressed by the three scintillator hodoscopes H1, H2, and H3 which are installed in the beam line (see fig.2).

Each hodoscope represents a thin sheet of scintillator material composed of 16 closely–packed scintillator rods. The rods in the first two hodoscopes are 1 cm wide and have a thickness of 5 mm in the direction of the beam, while the rods in H3 have a quadratic cross section of 6.5 mm × 6.5 mm. Width and thickness of the rods have been optimized to ensure sufficient light output from minimum–ionizing particles, while simultaneously maintaining the quality of the passing beam which is affected by multiple scattering. The rods are 10 cm long and are read out on either end by fast photomultipliers. A time resolution of 100 ps (1σ) has been realized with radioactive sources. In order to guarantee this time resolution also under beam conditions with particle rates up to 5×10^6 Hz, the photomultipliers are furnished with active voltage dividers that provide a stabilizing booster voltage at the last dynodes. Tracking calculations performed with the Monte Carlo program GEANT [3] show that the transmission losses introduced by the hodoscopes are less than 10% for momenta above 1 GeV/c and become significant only for considerably lower momenta.

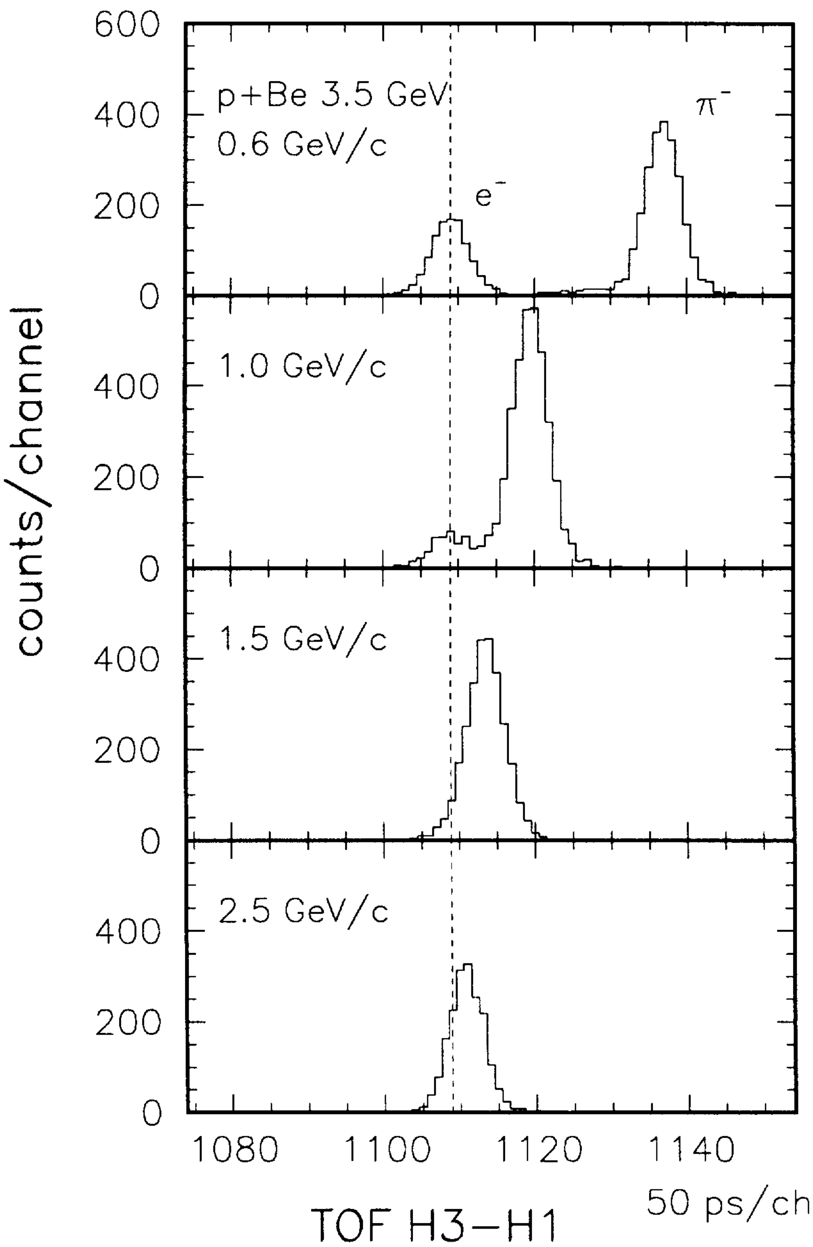

Figure 3: Time–of–flight difference between hodoscopes H3 and H1 as a function of the pre–selected momentum of the beam line. The spectra comprise all combinations of the 12 inner scintillator rods, the individual contributions being adjusted to coincide at the electron peak. The broken line refers to velocities $\beta = 1$.

Their modular structure endows the hodoscopes with a position resolution perpendicular to the direction of the rods which is given by $1/\sqrt{12}$ times the width of the rods. The time resolution, on the other hand, corresponds to a hit resolution of approximately 1 cm along the rods if one exploits the difference in the transit times of the correlated light signals. The refractive index of the scintillator material (Bicron BC404) is 1.58 and one has to assume an effective path which is longer than the straight distance because the light essentially propagates by internal reflection.

The momentum of the secondaries is measured by tracking the particles as they traverse the middle section of the beam line between the second and the third quadrupole doublet. Hodoscope H1 is mounted at the exit of the second doublet and H2 is mounted in the symmetric position at the entrance of the third doublet. In order to cope with the large horizontal and vertical emittances of the secondary particles their interception points with both H1 and H2 are used to determine the position in the image plane. With their rods oriented vertically the mid–section hodoscopes have an inherent position resolution of δx = 3.5 mm. The double position measurement in H1 and H2 thus transforms into a momentum resolution of δp/p$\leq$0.3% at the image plane.

Hodoscope H3 is located in the target section of the beam line behind the final quadrupole doublet. Its distance to the mid–plane hodoscopes is about 16 m and provides the baseline for time–of–flight measurements. Given a time resolution of 100 ps the identification of pions against protons and K mesons can be achieved over the full momentum range, while the separation of pions from electrons is only possible for momenta $\leq$ 800 MeV/c. The decay muons cannot be excluded quantitatively. Their flight times form a continuous distribution between the two extremes of pure pion and pure muon timing.

3 Commissioning of the pion beam

3.1 Experimental arrangement

The pion production runs were performed with primary beams at the maximum incident energy available, which was 3.5 GeV for protons and $2A$ GeV for ^{12}C. Prior to production, however, the performance of the beam line has been established with beams of lower energy.

Two ancillary detectors are installed near the HADES target point. The target detector, labelled TD in fig.2, is a plastic scintillator of hexagonal shape. It has a diameter of 10 cm and a thickness of 10 mm and fully intercepts the beam. The other detector is a two–dimensional array of 16$\times$32 scintillator fibers arranged horizontally and vertically, respectively. The fibers are of quadratic cross section with an area of 2$\times$2 mm^2. While the TD measures the total fluence of the secondary particles, the fiber array FA and the target hodoscope H3 together provide information on the beam profile in the vicinity of the target point.

3.2 Particle tracking

By following the individual particles along their trajectories it is possible to determine the momentum with an accuracy which is well within the acceptance window of the beam line. In order to investigate the tracking capability a primary proton beam of 1.6 GeV has been used with the production target being removed from its working position.

The direct beam from the synchrotron has a momentum resolution δp/p $\leq 10^{-3}$ and intrinsic horizontal and vertical emittances of 5π mm·mrad and 2π mm·mrad, respectively. In the course of the measurements the acceptance window was detuned by ±2% and ±5% with respect to the nominal value of 2.358 GeV/c. For each setting the x–positions in the image plane were determined by averaging the observed positions in H1 and H2. The excursions induced by the above variations do confirm the expected momentum dispersion of Δx/(Δp/p) = – 9 mm/%.

3.3 Pion identification

The pion beams are contaminated by like–sign particles. For π^- beams these are essentially electrons and negative muons, while protons occur in addition to positrons and positive muons in the case of positive polarity of the beam line.

As an example, fig.3 demonstrates the separation achieved for the negatively charged secondaries produced by a primary beam of 3.5 GeV protons. For a preselected momentum of 0.6 GeV/c, electrons and π^- are clearly separated, with μ^- contributing as a low–intensity shoulder on the high–velocity side of the π^- peak. Concerning the widths of the e^- and π^- peaks – both are 5 ± 0.5 channels – the status of the analysis is still controversial. Fact is that the momentum spread of the acceptance window introduces a velocity spread $\Delta\beta/\beta = (1/\gamma^2)\Delta$p/p. On the other hand, the laboratory resolution of 100 ps per phototube and the circumstance that time averages of the signals from either end of the rods are taken for the time–of–flight measurements are arguments to expect a 1σ time resolution of 100 ps, equivalent to 4.5 channels fwhm, for a sharp time spectrum. Thus electrons will produce an undistorted peak while the width of the pion distribution should show the influence of the momentum spread. With $1/\gamma^2$ = 0.0513 for pions of 0.6 GeV/c the contribution to be added in quadrature to the intrinsic resolution is 29 ps per percent Δp/p. Considering the statistical accuracy of the spectrum in fig.3 a contribution of 3 to 4 channels seems still consistent with the observed resolutions, resulting in an effective acceptance of Δp/p $\approx$ 6%. Extrapolation to a situation where hodoscope H1 is fully illuminated then leads to Δp/p = 8%. A more detailed discussion of the pion acceptance has to await further analysis of the data, where also the tracking information available from H2 is taken into account.

The high electron intensity at 0.6 GeV/c is remarkable. The electrons have their origin in the production target, coming mainly from conversion of high energy photons produced by $\pi^\circ \rightarrow \gamma\gamma$. For ^{12}C–induced production at 2A GeV and for the same acceptance window the e^-/π^- ratio drops from the present value of 0.45 to 0.15. The drastic change in the electron–to–pion ratio most likely is due to the different hardness of the pion spectrum produced in both cases.

As the acceptance window in fig.3 shifts to higher momentum the e^-/π^- ratio falls rapidly. At the same time the pions become more relativistic and start to override the electron intensity as evidenced by the time–of–flight differences of 11σ and 5σ at 0.6 and 1.0 GeV/c, respectively. In this situation a positive selection of the electrons could still be achieved with an additional threshold Čerenkov counter located between H1 and H2, see fig.2. Detector tests with electrons, for instance, could benefit from this possibility, especially if the electrons are enhanced by an additional photon converter at the production target.

3.4 Size of beam spot

First information about the size of the beam spot at the HADES target point is provided by a tracking analysis involving the target hodoscope H3 and the fiber array FA, see fig.2. The FA has a position resolution of 0.6 mm, both in x and in y direction, while H3, with its rods oriented horizontally, has 2.3 mm resolution in y but an uncertainty in x which is a factor of 4 to 5 larger.

Under the assumption that the focal point lies between both detectors, correlated hits give rise to trajectories which uniquely define the beam profile in the target section of the beam line. A particle–inclusive analysis of ^{12}C data at 1.5 GeV/c and for negative polarity of the beam line has given a minimum waist with 1σ dimensions of 0.5 cm in y direction and 1.0 cm in x direction at three quarters of the distance towards the FA. The uncertainty in x is dominated by the poor resolution of H3.

3.5 Pion intensities

During the commissioning the intensities of the primary beams were kept at 1–2×10^{10} particles per spill, with typical extraction times of 4 seconds from the synchrotron. The ions were provided by a conventional Penning source ($^{12}C^+$) and a multicusp ion source (H_3^+), respectively.

So far, production yields are available for negative pions only. The measurements have been performed with the target detector TD, which fully intercepts the beam at the HADES target point. The observed particle–inclusive intensities are corrected for the electron and μ^- contamination as estimated from the spectra in fig.3 and the equivalent ^{12}C–induced spectra. Potential users of the pion beam are interested in the maximum intensity at a given momentum. Therefore the observed yields are extrapolated to the space charge limit of the synchrotron, assuming ideal operation with 100% extraction efficiency, see tab.1.

The resulting yields are shown in fig.4. The ^{12}C–induced yields peak around 1 GeV/c. While the nearly exponential shape of the distribution at high momentum reflects the decreasing production cross section, the drop on the low–momentum

Table 1: Beam parameters for various ions accelerated by the synchrotron. In order to accelerate protons to energies above 3.5 GeV the transition point TP of the synchrotron has to be raised dynamically. The space charge limits, proportional to $\beta^2\gamma^3$, correspond to injection at 11.4A MeV and are given for an anticipated tuneshift spread of $\Delta Q = 0.2$. At the space charge limit projectiles with Z/A=1/2 represent a constant nucleon content of 2×10^{12}/spill. Future installation of corrective elements in the synchrotron might almost double ΔQ resulting in a boost of the space charge limits.

	p	d	^{12}C	^{20}Ne
max. kin. energy [GeV or A GeV]	3.5 4.7 (variable TP)	2.0	2.0	2.0
space charge limit [particles/spill]	5×10^{11}	1×10^{12}	1.7×10^{11}	1×10^{11}
permissible average intensity [particles/s]	1×10^{11} (at 3.5 GeV) 6×10^{10} (at 4.7 GeV)	6×10^{10}	6×10^{10}	6×10^{10}

side has its origin in the loss of pions due to decay in flight. The observed distribution is in qualitative agreement with simulations based on π^- production cross sections measured under 0° in Ne+NaF at 1.94A GeV, see ref.[4].

The proton–induced momentum distribution is much wider and the integral yield is lower than the ^{12}C–induced yield despite of the higher incident energy. The lower yield has to do with the smaller nucleon content of the synchrotron spill and also with the isospin asymmetry of the p+Be system which disfavours π^- production. For hard pions, however, the production exceeds the ^{12}C–induced intensities because of the higher energy per nucleon.

The maximum proton kinetic energy available from the 18 Tm synchrotron is 4.7 GeV. Above 3.5 GeV, however, stable acceleration is only possible if the optics of the synchrotron ring is changed dynamically from a 12fold symmetric pattern to 6fold symmetry. By this operation the transition point of the synchrotron is shifted upwards to higher energies. Extrapolation of the proton–induced 3.5 GeV results in fig.4 suggests that 4.7 GeV protons could very well be the beam of choice, especially for positive pions at high momentum. In the mean time the acceleration of protons to 4.7 GeV has been established in the synchrotron.

The proton and ^{12}C beam intensities used for the commissioning stayed well below the space charge limit of the synchrotron. Primary beams with intensities at the space charge limit have to await the installation of the high current injector which is scheduled for the second half of 1999. Even then, high intensity proton beams will be problematic due to the small mass–to–charge ratio of the

H_3^+ molecule used in the ion source. The cut–off values in the permissible average intensity (see tab.1) represent an additional limitation for proton–induced production. In order to exhaust the space charge limit, the proton experiments have to work with cycle times of 5 or 8 seconds, respectively. No limitation in this respect exists in the ^{12}C case. The present ramping speed of the synchrotron magnets does confine the change in rigidity to 13 Tm/s resulting in a minimum cycle time slightly below 4 seconds if one assumes an extraction time of 1 second.

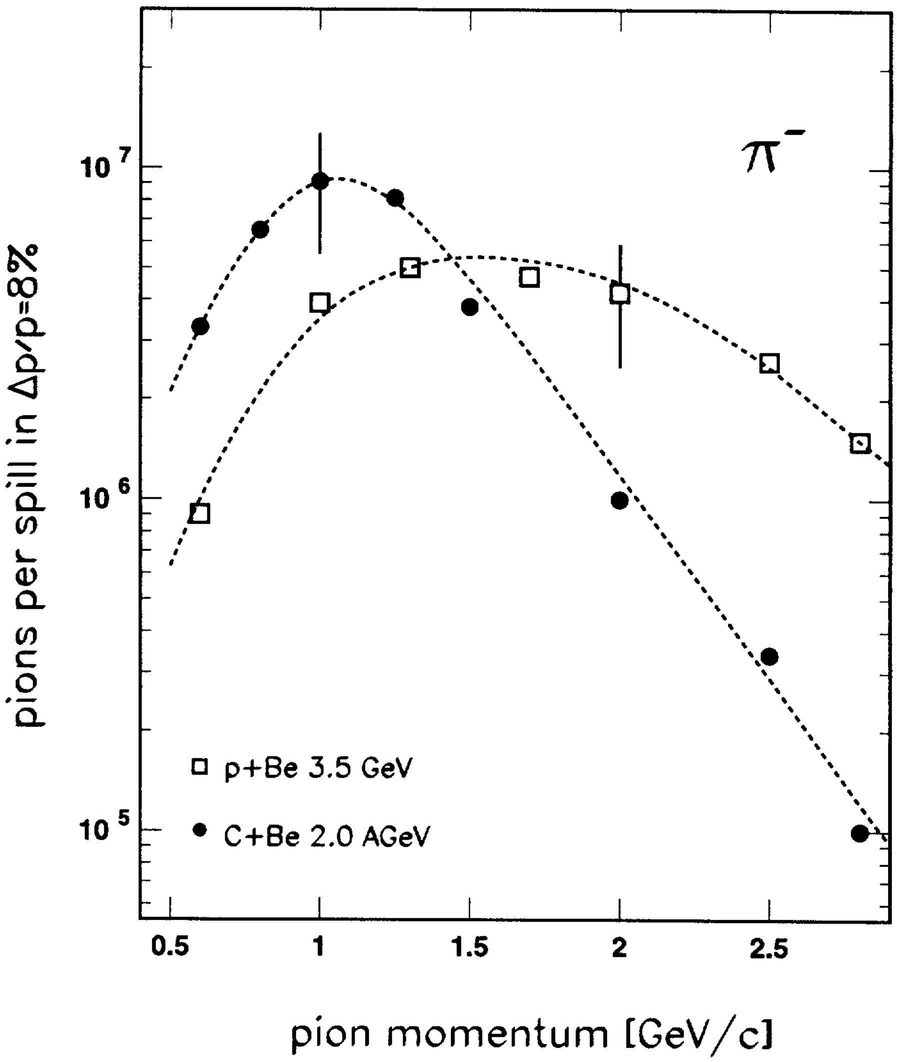

Figure 4: Maximum yields of negative pions expected at the HADES target point, as a function of the pion momentum selected by the acceptance window of the beam line. The momentum distributions are extrapolated to the space charge limit of the synchrotron using yields measured at primary beam intensities of 1 – 2 × 10^{10} particles/spill. The error bars (± 40%) comprise statistical as well as systematic contributions and reflect the uncertainty of the present, still preliminary analysis.

4 Conclusion

In order to complement the physics program at the heavy–ion synchrotron, GSI has recently installed a low–momentum secondary beam facility which primarily aims at pion production. The secondary beams can be delivered to all major experimental areas in the SIS target hall. The commissioning with negative pions took place in the new beam line to the HADES cave. Thirty–three meters long, the line accomodates pion momenta up to 2.8 GeV/c and has a momentum acceptance of $\Delta p/p$=8%. Tracking provides a momentum resolution of 0.3% within the acceptance window.

For ^{12}C projectiles with the maximum SIS energy of 2A GeV the negative pion yields at the HADES target point reach values of 1×10^7/spill near the peak of the momentum distribution around 1 GeV/c, if extrapolated to the space charge limit of the synchrotron. With beryllium as the production target, the collision system is nearly isospin–symmetric and positive and negative pions are equally abundant. The corresponding proton–induced yields of negative pions at 3.5 GeV incident energy are smaller except for hard pions for which the production exceeds the ^{12}C–induced intensities because of the higher energy per nucleon. By special operation – not yet required at 3.5 GeV – the transition point of the synchrotron can be shifted up dynamically to realize proton energies up to 4.7 GeV. Protons of this energy are expected to be the beam of choice for positive pions and for pions with high momentum.

The pion beam facility was realized in the framework of a collaboration comprising the laboratories GANIL and GSI as well as the universities of Gießen, Lund, and Valencia. The project is being supported by the European Community TMR–LSF RTD Programme, contract no. ERBFMGECT950009.

References

[1] K.H. Kanaka et al., Nucl. Instr. and Meth. in Phys. Res. A363(1995)114.

[2] B.M. Abramov et al., Nucl. Phys. A372(1981)301.

[3] GEANT 3.21, CERN program library W5013, CERN Geneva.

[4] A. Gillitzer et al., Z. Phys. A354(1996)3.

Invited talk presented at the Erice Summer School of Nuclear Physics, September 17 – 25, 1998, Erice, Italy.
To be published in Progress in Particle and Nuclear Physics, Elsevier Science.